Dielectric spectroscopy of cosurfactant facilitated percolation in reverse microemulsions

Yuriy Alexandrov, Nick Kozlovich, Yuri Feldman, and John Texter

Citation: The Journal of Chemical Physics **111**, 7023 (1999); doi: 10.1063/1.479994
View online: http://dx.doi.org/10.1063/1.479994
View Table of Contents: http://scitation.aip.org/content/aip/journal/jcp/111/15?ver=pdfcov
Published by the AIP Publishing

Dielectric spectroscopy of cosurfactant facilitated percolation in reverse microemulsions

Yuriy Alexandrov, Nick Kozlovich, and Yuri Feldman
Department of Applied Physics, The Hebrew University of Jerusalem, 91904 Jerusalem, Israel

John Texter
Strider Research Corporation, Rochester, New York 14610-2246

(Received 4 December 1998; accepted 26 July 1999)

Percolation in reverse microemulsion systems can be driven by various field variables, including temperature and cosurfactant concentration. We use dielectric spectroscopy and a macroscopic dipole correlation function (DCF) derived therefrom to examine mesoscale structural aspects of charge transport in a water, AOT, toluene reverse microemulsion that is driven into percolation by cosurfactant (acrylamide). A multiexponential fitting of the DCF data gives firm support to the importance of a parameter marking the onset of percolation, as distinguished from the percolation threshold. A stretched exponential fitting of the DCF data reveals microstructural and mesoscale similarities and differences between this case of cosurfactant-induced percolation and a previously examined case of temperature-induced percolation. This cosurfactant-driven system appears to exhibit a critical slowing down on approach to the percolation threshold, as does the temperature-driven case, but a much shorter relaxation time suggests the development of much less fractal structure in this cosurfactant case. The effective fractal dimensionality and number of self-similarity stages of the fractal structure are only weak functions of the reduced field variable in the case of cosurfactant-driven percolation, and contrast sharply with the temperature case.
 [S0021-9606(99)71839-8]

I. INTRODUCTION

Percolation phenomena are induced in water-in-oil microemulsions by a variety of field variables, including disperse phase volume fraction, the ratio of water to surfactant, temperature, or chemical potential in some additive or fourth chemical component.[1–5] Various additives have been shown to retard percolation, and others have been shown to facilitate percolation.[6,7] Acrylamide, other primary amides, and acetonitrile have been shown to function as cosurfactants in water, AOT, toluene reverse microemulsions and to facilitate percolation phenomena in such microemulsions.[8,9] This percolation phenomenon appears to correspond to the formation of percolating clusters of droplets from isolated microemulsion droplets or to the formation of percolating networks from nonpercolating clusters of droplets.

This percolation has been manifested by a rapid increase in the electrical conductivity of the microemulsion when the cosurfactant concentration ξ reaches a critical value, ξ_p, the percolation threshold, at a constant temperature. In this case the cosurfactant concentration is a monotonic function of the field variable, chemical potential ($RT \ln \xi$). This rapid variation in electrical conductivity in the neighborhood of the threshold ξ_p can be represented by two well-known scaling laws,

$$\sigma \propto (\xi_p - \xi)^{-s} \quad \text{for} \quad \xi_p > \xi, \tag{1}$$

and

$$\sigma \propto (\xi - \xi_p)^{t} \quad \text{for} \quad \xi > \xi_p, \tag{2}$$

with critical exponents $s = 0.69$ and $t = 1.49$.[8,9]

Two models, static percolation and dynamic percolation, have been proposed to account for percolation in electrical conductivity in reverse microemulsions. The static percolation model envisions the formation of connected water paths in the system.[10] The dynamic percolation model envisions connected charge carrier trajectories through clusters, but where the trajectories need not be instantaneously supported by clusters except in the neighborhood of the charge carrier.[11] In this dynamic picture, charge transport is assured by the hopping or diffusing of charge carriers through clusters that rearrange with time. The static percolation limit has exponents $s \approx 0.7$ and $t \approx 1.9$, whereas dynamic percolation yields exponents $s \approx 1.2$ and $t \approx 1.6–1.9$.[1,3]

In the case of temperature-induced percolation it was shown[1] that below the percolation threshold dynamic percolation takes place ($s \approx 1.2$). This percolation corresponds to transport of counterions within transient clusters.[12] These positive counterions are formed as a result of the limited dissociation of AOT to sodium cation and organic anion at the aqueous interface in the droplets.[13,14] Experiments have shown that this water–acrylamide–AOT–toluene system is not driven into percolation by temperature.[15] The magnitude of the $s = 0.69$ exponent derived for the cosurfactant-induced percolation appears closer to the 0.7 value, i.e., typical for the static limit. However, the analysis of the self-diffusion coefficients for water, acrylamide, and AOT in the water–acrylamide–AOT–toluene system does not provide any indication of the formation of bicontinuous microstructures.[8] Lengthy strings of droplet clusters may provide network sup-

port for static percolation without having to invoke irregular bicontinuous microstructure.

Among various physical methods which can provide information about the structure and dynamic processes that occur in microemulsions, dielectric spectroscopy is a tool that can probe different kinds of dynamics and morphologies.[16] In particular, time domain dielectric spectroscopy (TDDS) was recently used, over a wide temperature and frequency range, to determine significant temporal characteristics of ionic microemulsions at percolation.[1,2]

The aim of this work is to further investigate the structure and dynamic processes that occur in this water, acrylamide, AOT, and toluene microemulsion system, wherein percolation is driven by cosurfactant (concentration). Our approach rests upon the experimental and theoretical analysis of the macroscopic dipole correlation function (DCF) derived from dielectric spectroscopy measurements. We particularly wish to contrast results obtained for this example of cosurfactant driven percolation with the case of temperature-induced percolation analyzed earlier.[1,17]

II. EXPERIMENT

Reverse microemulsions of water, acrylamide, AOT, and toluene were prepared as described earlier.[18] The molar ratio of water, AOT, and toluene was kept fixed at 11.2:1.00:19.2, and acrylamide concentration ξ was varied over the range of 0–6% *(w/w)*. AOT, toluene and decane were purchased from Sigma and used without further purification. Deionized and twice distilled water was used throughout the experiments.

Dielectric measurements were done using a TDS-2 (Dipole TDS, Ltd., Jerusalem) time domain dielectric spectroscopy system in the frequency range 100 kHz–5 GHz. All measurements were performed at 25 °C. General principles of TDDS and a detailed description of the setup and procedures of measurements have been described elsewhere.[19] The data treatment was carried out directly in the time domain in terms of the macroscopic dipole correlation functions (DCF). The DCF contains all the information on the dynamics of all dipolar species in the system. The least-squares fitting procedure used was based on the simulated annealing method.[20] Low frequency electrical conductivity was measured using a conductivity meter manufactured by Radiometer (Copenhagen).

III. RESULTS

Low frequency dielectric permittivity and electrical conductivity for this water, AOT, toluene microemulsion system as a function of added acrylamide (ξ) are shown in Fig. 1. The conductivity, σ, increases almost three orders of magnitude due to a fivefold increase in acrylamide concentration. The static permittivity exhibits a relative maximum over this same interval. The percolation threshold in electrical conductivity, $\xi_{p\sigma}$, is normally defined as the inflection point in such a semilogarithmic curve. The relative maximum illustrated in the static permittivity defines a percolation threshold in permittivity, $\xi_{p\epsilon}$.[1] These thresholds do not necessarily closely coincide. These data and respective thresholds serve to define three intervals: below percolation threshold with $\xi < \xi_{p\sigma}$, in the vicinity of threshold with $\xi_{p\sigma} < \xi < \xi_{p\epsilon}$, and above threshold with $\xi > \xi_{p\epsilon}$.

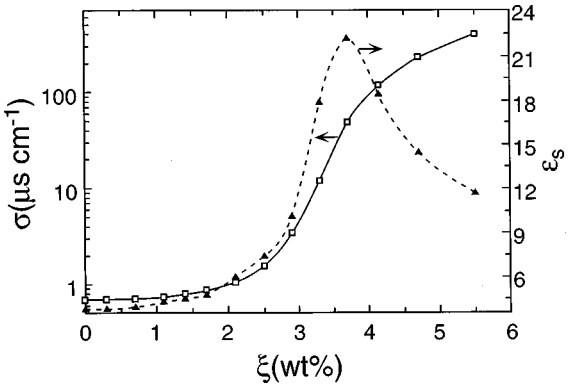

FIG. 1. Low frequency conductivity and static dielectric permittivity of the water, acrylamide, AOT, toluene reverse microemulsion system at 25 °C as a function of acrylamide concentration (wt. %).

The macroscopic dielectric correlation (relaxation) function $\Psi(t,\xi)$ for this system is illustrated in Fig. 2 for times up to 50 ns and for the 0–5% *(w/w)* range in acrylamide, ξ. One can see that the DCF displays complex nonexponential behavior. The DCF decay dynamics vary dramatically with ξ. This behavior is reminiscent of similar data obtained for a case of temperature driven percolation.[17]

IV. DISCUSSION

An earlier discussion of the scaling behavior of these conductivity data has been reported.[8,9] We note here that the electrical conductivity percolation threshold yielded $\xi_{p\sigma} \approx 3.1\%$. Another important parameter is the onset of electrical percolation, ξ_o, obtained as a breakpoint in the toe region of the (log) conductivity-ξ curve. This parameter ξ_o marks the onset of percolating cluster formation or the onset of

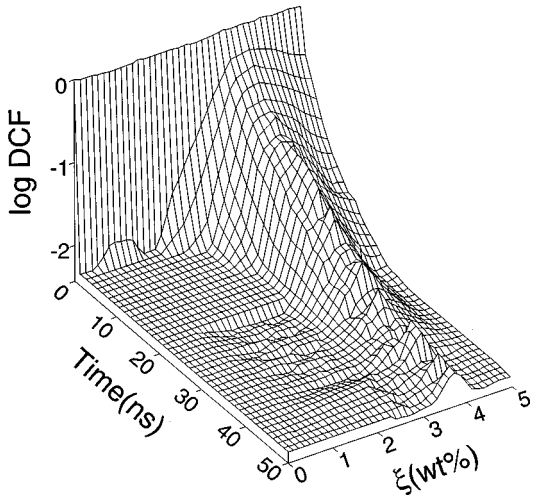

FIG. 2. Perspective plot of the time and acrylamide (cosurfactant) weight percent dependencies of the macroscopic dipole correlation function (DCF) for the water, acrylamide, AOT, toluene reverse microemulsion system at 25 °C.

percolation in nonpercolating clusters. The percolation threshold in static permittivity obtained in an earlier analysis yielded $\xi_{p\epsilon} \approx 3.7\%$.

Below ξ_o the microemulsion consists of isolated reverse microemulsion water droplets in equilibrium with nonpercolating clusters of droplets. Hence, to a good approximation the dielectric permittivity of this system can be described in terms of a fluctuation mechanism of dielectric polarization.[13,14] According to this mechanism, the droplet polarizability is proportional to the mean-square fluctuation dipole moment of the droplet. The mean-square dipole moment and the corresponding value of the dielectric increment depend on the equilibrium distribution of counterions within a diffuse double layer. The density distribution of ions is determined by the degree of the dissociation of the ionic surfactant.

When ξ increases above ξ_o (1.2%) and reaches the permittivity percolation threshold $\xi_{p\epsilon}$ (3.7%), the static dielectric permittivity ϵ increases in accordance with the following scaling law:

$$\epsilon \propto (\xi_{p\epsilon} - \xi)^{-s} \quad \text{for} \quad \xi < \xi_{p\epsilon}, \tag{3}$$

with critical exponent $s = 0.7$. This result is very close to the numerical value obtained from our conductivity measurements and agrees well with the value predicted by the static percolation model.

In the limit of low ξ where the microemulsion structure is predominantly isolated spherical droplets, the conductivity and the static dielectric permittivity are almost linearly proportional to ξ. The ensuing behavior of ϵ and σ with increasing ξ can be described by the fluctuation mechanism of dielectric polarization[13,14] and the charge fluctuation mechanism[21,22] for ϵ and σ behavior, respectively. In the charge fluctuation model, the conductivity is explained by the migration of charged aqueous non-interacting droplets in the electric field. The droplets acquire charges owing to the fluctuating exchange of charged surfactant heads at the droplet interface and the appositely charged counterions in the droplet interior. We can also speculate that the very small increases in ϵ and σ with increasing ξ at low ξ may be due to the increase in the disperse phase volume fraction attendant to increasing ξ.

Increasing ξ leads to increases in the fluidity (decreasing rigidity) of the interface and results in an increase in the attractive interaction between droplets. This increasing attractive interaction facilitates merging of the droplets and the formation of droplet clusters.[23,24] Since the cosurfactant incorporates into the dispersed aqueous phase, the disperse phase volume fraction increases concomitantly with increasing cosurfactant concentration. The water-swollen micelles (microemulsion droplets) play the role of the structural units which are built upon to form the clusters. This sequential aggregation to form large clusters or strings of droplets leads to formation of mesoscale inhomogeneities in the system. Such mesoscale inhomogeneities can be described by fractal models.[17,25,26]

A dynamical analysis can yield information about the mesoscale morphology. In order to understand the dipole correlation function behavior (Fig. 2), it is necessary to analyze several possible sources of dielectric relaxation and polarization. These sources include the movement of surfactant counterions relative to the negatively charged droplet interface, reorientation molecular motions of the AOT anion, reorientation of acrylamide, and reorientation of free and bound water molecules.

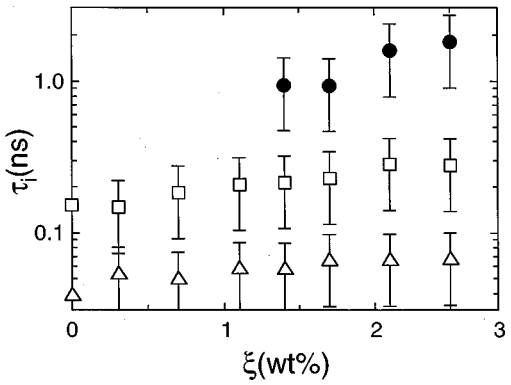

FIG. 3. Relaxation times derived by fitting the macroscopic dipole correlation function (DCF) data of Fig. 2 to Eq. (4) for the water, acrylamide, AOT, toluene reverse microemulsion system at 25 °C, τ_1, △; τ_2, □; τ_3, ●.

Below the onset of percolation, for $\xi < \xi_o$, the main contribution in the relaxation mechanism comes from the processes that are inherent to the dynamics of an isolated droplet. The DCF in this region also exhibits nonexponential behavior. Since the polarization of droplets far below the percolation threshold is the superposition of several independent mechanisms, DCF can in a first approximation be represented by the formal sum of N Debye-type relaxation processes as

$$\Psi(t) = \sum_{i=1}^{N} A_i \exp(-t/\tau_i), \tag{4}$$

where

$$\sum_{i=1}^{N} A_i = 1, \tag{5}$$

where the τ_i are the relaxation times and the A_i are the amplitudes of the relaxation processes.

The results of the fitting of the experimental DCF according to Eq. (4) are shown in Figs. 3 and 4. Two terms, τ_1 and τ_2, appear sufficient to fit the observed relaxation for $\xi < \xi_o$. The relaxation times for these processes range over 0.04–0.07 ns for τ_1 and over 0.15–0.3 ns for τ_2. As the acrylamide concentration surpasses ξ_o, the minimum number of elementary Debye processes required to fit the data is three. The appearance of this longer relaxation process at $\xi \approx \xi_o$ with a characteristic time τ_3 ranging from about 1 to 2 ns closely coincides with the onset of percolation. It should, therefore, have a cooperative nature. We suggest that the strong dielectric response above ξ_o, reflected by the increase of the amplitude A_3 of this cooperative process (Fig. 4), is associated with the transfer of charge carriers along the aggregate clusters and mesoscale structures. Transport of electrical charges along droplet clusters modifies the total fluctuation dipole moment. This moment comprises the

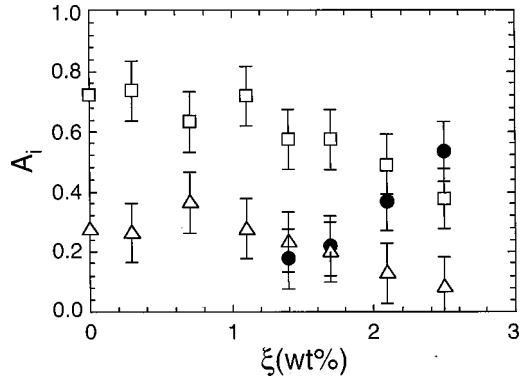

FIG. 4. Relaxation amplitudes derived by fitting the macroscopic dipole correlation function (DCF) data of Fig. 2 to Eq. (4) for the water, acrylamide, AOT, toluene reverse microemulsion system at 25 °C; A_1, △; A_2, □; A_3, ●.

individual fluctuating dipoles from each droplet. Both the amplitude and the relaxation time of this process follow the increase of the spatial scale of charge separation in the system with increasing magnitude of the connectivity length.[27]

The two faster relaxation processes (relaxation times τ_1 and τ_2 and amplitudes A_1 and A_2) persist above ξ_o. These relaxation times are distributed within the ranges of dozens and hundreds of ps, respectively. The fastest relaxation process (τ_1,A_1) presumably is related to the relaxation and reorientation of bound water, AOT anion, and or acrylamide molecules. The intermediate process (τ_2,A_2) is related to the concentration polarization mechanism[13,14] associated with fluctuations of the ionic density due to the movements of ions (charge carriers).

Since the longest relaxation process (τ_3,A_3) reflects the cooperative dynamics in the system at percolation, its analysis can provide information about the morphology and dynamics on a mesoscale. This information can be inferred with the help of a recursive fractal model of cooperative dielectric relaxation[17] introduced earlier. According to this model, the description of the morphology in a self-similar medium may be approximated by the discrete scaling

$$L_j = \lambda b^j, \tag{6}$$

where L_j is the effective length of (a channel of) the relaxation trajectory in the jth stage of self-similarity, λ is the minimal scale (size of the structural unit), and b is a scaling factor ($b>1$). The jth stage is considered with respect to the reference unit being the zeroth stage.

The total number of units related to the jth stage of self-similarity (i.e., located at a distance L_j from the reference unit) is scaled as

$$n_j = n_0 p^j, \tag{7}$$

where p is the scaling factor ($p>1$), and n_0 is the number of the nearest neighbors near the selected droplet or unit (i.e., $j=0$).

According to this model, the probability of the structural unit remaining polarized in a cluster having j stages of self-similarity is described by a ''microscopic survival probability function'' $g(z/z_j)$. In this function z_j is a time variable characterizing the jth stage of the self-similarity, z is a dimensionless time ($=t/\tau'$), where τ' is the minimal relaxation time of separated structural units.[23,28] The following scaling assumption is invoked:

$$z_j = aL_j^E = a(\lambda b^j)^E = a\lambda^E k^j, \tag{8}$$

where the parameter k equals b^E. Here, a is a proportionality coefficient, and E is the scaling index that coincides with the space dimensionality. The assumption that $E=3$ constitutes a conjecture on the proportionality of characteristic relaxation time to the magnitude of the characteristic volume.[23,29]

This model makes it possible to express the full time-dependent probability for the structural unit to remain in its polarized state (in the effective fractal structure having N stages of self-similarity), as the *product* of microscopic survival probability functions. This probability coincides with the total time-dependent DCF.[30] This product relationship for the DCF may be written as

$$\Psi_N(z) = \prod_{j=0}^{N} [g(z/z_j)]^{n_j} = \prod_{j=0}^{N} [g(Z\xi^j)]^{n_0 p^j}, \tag{9}$$

where $Z=t/(a\lambda^E\tau_1)$, $\xi=1/k$, and $N=\ln(L_N/\lambda)/\ln k$. Here L_N is the finite geometrical size of the fractal cluster, where N refers to the last stage of self-similarity.

The product in Eq. (9) may be estimated for various values of $\xi<1$ and $p>1$ (see Ref. 17). The results of these estimates may be written in the form of a modified Kohlrausch–Williams–Watts (KWW) stretched-exponential relaxation law,

$$\Psi(Z) = A\ \exp\{-\Gamma Z^\nu + BZ\}, \tag{10}$$

where

$$A = \left(\frac{1}{\overline{g}}\right)^{-\theta}, \tag{11}$$

with $\theta = n_0(1/2+1/\delta)$ and $\delta = \ln(1/\xi)$,

$$\Gamma = \frac{n_0}{\ln(1/\xi)} \int_0^\infty y^{-\nu} \left| \frac{g'(y)}{g(y)} \right| dy, \tag{12}$$

$$B = \frac{n_0 a_1}{\ln(1/\xi)(1-\nu)} \epsilon^{1-\nu}, \tag{13}$$

and

$$\nu = \ln p / \ln(1/\xi), \tag{14}$$

with $0<\nu<1$ and for $\epsilon = \xi^N \ll 1$.

The parameters $\overline{g}$, A_1, a_1, and a_2 in Eqs. (11)–(14) are related to the asymptotic properties of the elementary relaxation function $g(y)$,[17]

$$g(y) = 1 - a_1 y + a_2 y^2 + \cdots \quad \text{for} \quad y \ll 1; \tag{15}$$

$$g(y) = \overline{g} + A_1/y + A_2/y^2 + \cdots \quad \text{for} \quad y \gg 1. \tag{16}$$

The parameter Γ in Eq. (10) depends on the function $g(y)$ and affects the macroscopic relaxation time $\tau = \tau' a \lambda^E \Gamma^{-1/\nu}$. B is a correction for the KWW function at large times.

The relationship between the exponent ν and the fractal dimension D_f may be derived from the proportionality and

scaling relations. The number of droplets (units) which belong to all of the self-similarity stages, including the jth stage (size of an effective cluster), is scaled as $S_{\mathrm{eff}}=N_j\sim p^j$,

$$S_{\mathrm{eff}}=N_j=\sum_{k=0}^{j} n_k=\sum_{k=0}^{j} n_0 p^k=n_0^2\frac{p^{i+1}-1}{p-1}$$

$$\approx\left(\frac{n_0^2 p}{p-1}\right)p^j, \quad \text{for} \quad j\gg 1. \tag{17}$$

On the other hand, the definition of the ''mass fractal dimension'' D_f (Ref. 31) provides that

$$N_j\sim L_j^{D_f}. \tag{18}$$

Taking the logarithm of this expression and incorporating the relations from Eqs. (6) and (7), one obtains

$$D_f=\ln p/\ln b=E\nu, \quad \text{for} \quad E=3. \tag{19}$$

In order to fit the experimental data according to this cooperative relaxation model,[17] it is necessary to estimate the values of the minimal temporal scale τ', and the minimal spatial scale (structural unit size) λ. The value of τ' is the characteristic time of the elementary relaxation process occurring at the level of a structural unit. The value $\tau'=0.45$ ns was chosen for the minimal temporal scale. This value corresponds to the characteristic time τ_2 resolved earlier for the relaxation of the polarization of the diffuse counterion layer in the droplet interior at low ξ. The minimal structural unit in the fitting procedure was chosen as a scaled parameter. It changes as long as the system approaches the percolation threshold.

A detailed discussion of the application of this recursive fractal model to the analysis of temperature-driven percolation in water, AOT, decane microemulsions was given earlier.[17] This same algorithm has been applied here to this water, AOT, acrylamide, toluene microemulsion system. The experimentally measured DCF were fitted to the relaxation law predicted by the theory in the form of Eq. (10). The fitting parameters were p, k, n_0, N, and $D_f(a\lambda^E)^{-1}$. The data were averaged over many fitting cycles. For each point, a minimum of two independent TDDS relaxation measurements were made.

The values of the macroscopic relaxation time τ and of the morphological parameters D_f and N obtained from the fitting of our experimental DCF data to Eq. (9) are illustrated in Figs. 5, 6, and 7, respectively. In these figures we plot the behavior of τ, D_f, and N as functions of a master coordinate $(x-x_p)/x_p$ for $x=\xi$ and T. We present the data obtained from fitting the DCF illustrated in Fig. 2 for cosurfactant-induced (ξ) percolation, and we present data taken from Ref. 17 that were obtained for a case of temperature-induced percolation.

The behavior of the macroscopic effective relaxation time τ as a function of $(x-x_p)/x_p$ illustrated in Fig. 5 exhibits a maximum and resembles a critical slowing down in both of these systems.[27] One can see that the relative macroscopic relaxation time at the percolation onset has the same value. However, at the percolation threshold, the value of the relaxation time in the case of the temperature-induced percolation is ten times higher than the value of the relaxation time for the acrylamide-facilitated percolation. This means that the droplet clusters in this cosurfactant-containing system are

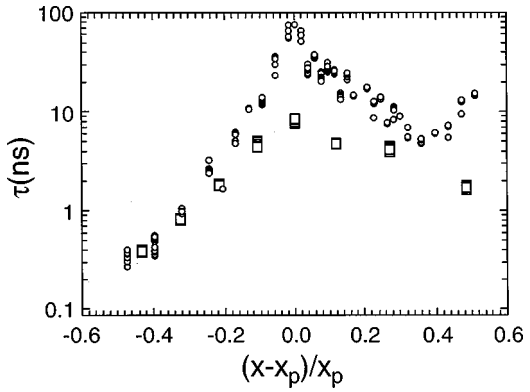

FIG. 5. Master plot of the macroscopic effective relaxation time defined in the cooperative relaxation (CR) model for acrylamide-induced (□) and temperature-induced (○) percolation. In the case of the acrylamide data, × corresponds to ξ, cosurfactant concentration (wt. %). In the case of the temperature data, × corresponds to T.

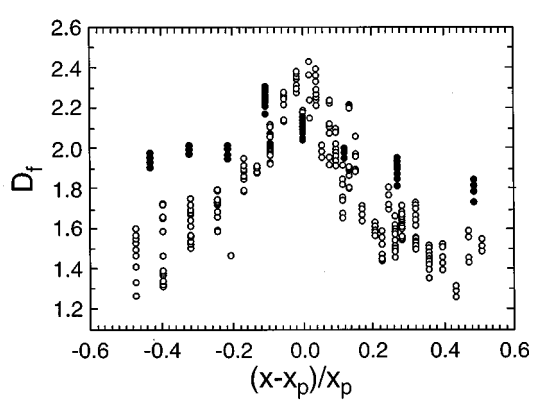

FIG. 6. Master plot of the effective fractal dimension defined in the CR model for acrylamide-facilitated (●) and temperature-facilitated (○) percolation.

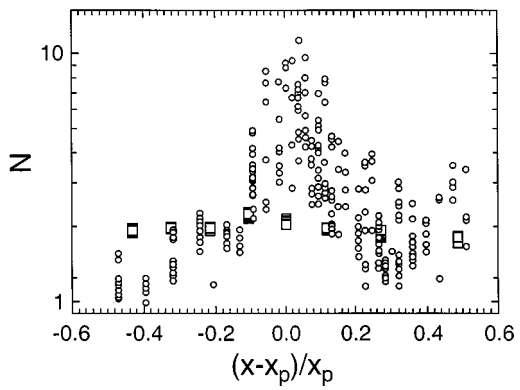

FIG. 7. Master plot of the maximal number of self-similarity stages defined in the CR model for acrylamide-facilitated (□) and temperature-facilitated (○) percolation.

not so well developed as in the temperature-facilitated percolation case.

The behavior of the effective fractal dimension D_f illustrated in Fig. 6 shows that the fractal dimension in the acrylamide system only weakly changes as a function of ξ. This dimensionality varies between 1.9 and 2.2 with an error margin of approximately 0.1. The comparative values of the fractal dimension D_f for the temperature-induced percolation (filled symbols) appear smaller at the onset of percolation and far above the threshold, with D_f in the range of 1.3–1.6. However, both processes yield values of 2.1–2.3 in the neighborhood of the threshold. The number of self-similarity stages illustrated in Fig. 7 exhibits an even greater contrast between the cosurfactant driven case (open squares) and the temperature-induced percolation data (open circles). The number of self-similarity stages for cosurfactant-driven percolation has a relatively small value, about 2, and appears not to depend on ξ. This small value of N means that the fractality is weakly developed. In order to explain the insensitivity of N to ξ (acrylamide content) along with the strong dependence of the relaxation time τ on ξ, one could suppose that the minimal spatial scale λ and minimal temporal scale τ' increases as long as ξ increases. This supposition means that the structural unit might *change* when ξ increases. Hence, if at the percolation onset a structural unit of the fractal was considered a single droplet, then when the system approaches the percolation threshold, the structural unit might represent already a cluster, consisting of enchained droplets.

V. CONCLUSIONS

The transition marker ξ_o has been defined experimentally as a breakpoint in the water self-diffusion coefficient,[7,9] as a breakpoint in the electrical conductivity signaling the onset of percolation,[7,9] and as a breakpoint in Faradaic electron transfer observed electrochemically.[9,32] The present results of Figs. 3 and 4 show that this onset of cooperativity is also signaled by the appearance of a third relaxation mode at $\xi > \xi_o$. This relaxation mode establishes firm empirical basis for ξ_o as a transition marker distinguishable from the percolation threshold ξ_p.

Our analysis of the macroscopic dipole correlation function in terms of our recursive fractal model permits us to make a detailed comparison of the percolation driven by acrylamide (cosurfactant chemical potential) in this water in toluene system with the percolation driven by temperature in a water in decane system.[7,9] We make this comparison in terms of three key parameters, the macroscopic relaxation time (τ), the fractal dimension (D_f), and the number of self-similarity stages *(N)*. This comparison is facilitated by using the reduced intensive variable $(x-x_p)/x_p$ for $x=\xi$ (cosurfactant concentration) and T (temperature).

The comparison in Fig. 5 of the macroscopic relaxation time, τ, shows that both systems share qualitative commonality. Both systems exhibit a critical slowing down on approach to the percolation threshold. This long relaxation time obtained with cosurfactant (acrylamide) driven percolation, however, is tenfold smaller than that obtained in the temperature driven system. This smaller relaxation time indicates that charge transport along fractal clusters is damped to a greater degree in this acrylamide-containing system.

The minor variation with reduced intensive variable $(\xi-\xi_p)/\xi_p$ in D_f (Fig. 6) and the small number of self-similarity stages N (Fig. 7) obtained for this cosurfactant driven system show that cluster formation and transport is much less fractally developed than in the comparison temperature-driven system.

[1] Yu. Feldman, N. Kozlovich, I. Nir, and N. Garti, Phys. Rev. E **51**, 478 (1995).
[2] C. Cametti, P. Codastefano, P. Tartaglia, S. Chen, and J. Rouch, Phys. Rev. A **45**, R5358 (1992).
[3] J. P. Clerc, G. Giraud, J. Laugier, and J. Luck, Adv. Phys. **39**, 191 (1990).
[4] M. A. Dijk, G. Casteleijn, J. G. H. Joosten, and Y. K. Levine, J. Chem. Phys. **85**, 626 (1986).
[5] C. Boned, J. Peyrelasse, and Z. Saidi, Phys. Rev. E **47**, 468 (1993).
[6] J. Texter, in *Nonequilibrium Dynamic Processes at Colloidal Interfaces*, edited by Y. Shnidman (ACS, Washington, DC, in press).
[7] J. Texter, Colloids Surfaces A Phys. Eng. Aspects (in press).
[8] B. Antalek, A. J. Williams, J. Texter, Yu. Feldman, and N. Garti, Colloids Surf., A **128**, 1 (1997).
[9] J. Texter, B. Antalek, E. García, and A. J. Williams, Prog. Colloid Polym. Sci. **103**, 160 (1997).
[10] P. G. DeGennes and C. Touplin, J. Phys. Chem. **86**, 2294 (1982).
[11] G. Grest, I. Webman, S. Safran, and A. Bug, Phys. Rev. A **33**, 2842 (1986).
[12] Yu. Feldman, N. Kozlovich, I. Nir, N. Garti, V. Archipov, Z. Idiyatullin, Y. Zuev, and V. Fedotov, J. Phys. Chem. **100**, 3745 (1996).
[13] N. Kozlovich, A. Puzenko, Yu. Alexandrov, and Yu. Feldman, Colloids Surf., A **140**, 299 (1998).
[14] N. Kozlovich, A. Puzenko, Yu. Alexandrov, and Yu. Feldman, Phys. Rev. E **58**, 2179 (1998).
[15] Yu. Feldman, Yu. Alexandrov, and N. Kozlovich (unpublished).
[16] A. K. Jonscher, *Dielectric Relaxation in Solids* (Chelsea Dielectric, London, 1983).
[17] Yu. Feldman, N. Kozlovich, Y. Alexandrov, R. Nigmatullin, and Y. Ryabov, Phys. Rev. E **54**, 5420 (1996).
[18] E. García, S. Song, L. E. Oppenheimer, B. Antalek, A. J. Williams, and J. Texter, Langmuir **9**, 2782 (1993).
[19] Yu. Feldman, A. Andrianov, E. Polygalov, G. Romanychev, I. Ermolina, and Y. Zuev, Rev. Sci. Instrum. **67**, 3208 (1996).
[20] R. Lisin, B. Ginzburg, M. Schlesinger, and Yu. Feldman, Biochim. Biophys. Acta **1280**, 34 (1996).
[21] H. F. Eicke, M. Borkovec, and B. Das-Gupta, J. Phys. Chem. **93**, 314 (1989).
[22] D. G. Hall, J. Phys. Chem. **94**, 429 (1990).
[23] L. Garcia-Rio, J. R. Leis, J. C. Mejuto, M. E. Pena, and E. Iglesias, Langmuir **10**, 1676 (1994).
[24] W. Gelbart and A. Ben-Shaul, J. Phys. Chem. **100**, 13169 (1996).
[25] R. Hilfiker and H. F. Eicke, J. Chem. Soc., Faraday Trans. 1 **83**, 1621 (1987).
[26] S. H. Chen, J. Rouch, F. Sciortino, and P. Tartaglia, J. Phys.: Condens. Matter **6**, 10855 (1994).
[27] D. Stauffer and A. Aharony, *Introduction to Percolation Theory*, 2nd ed. (Taylor and Francis, London, 1994), p. 8.
[28] C. Cametti, F. Sciortino, P. Tartaglia, J. Rouch, and S.-H. Chen, Phys. Rev. Lett. **75**, 569 (1995).
[29] V. Degiorgio, R. Piazza, F. Mantegazza, and T. Bellini, J. Phys.: Condens. Matter **2**, SA69 (1990).
[30] N. Goldenfeld, *Lectures on Phase Transitions and the Renormalization Group* (Addison–Wesley, New York, 1992), p. 132.
[31] E. Feder, *Fractals* (Plenum, New York, 1988), Chap. 7.
[32] E. García and J. Texter, J. Colloid Interface Sci. **162**, 262 (1994).